

# World Journal of *Gastrointestinal Surgery*

*World J Gastrointest Surg* 2022 October 27; 14(10): 1089-1178



**REVIEW**

- 1089 Drain fluid biomarkers for prediction and diagnosis of clinically relevant postoperative pancreatic fistula: A narrative review  
*Rykina-Tameeva N, Samra JS, Sahni S, Mittal A*

**ORIGINAL ARTICLE****Retrospective Study**

- 1107 Performing robot-assisted pylorus and vagus nerve-preserving gastrectomy for early gastric cancer: A case series of initial experience  
*Zhang C, Wei MH, Cao L, Liu YF, Liang P, Hu X*
- 1120 Long-term efficacy and safety of cap-assisted endoscopic sclerotherapy with long injection needle for internal hemorrhoids  
*Xie YT, Yuan Y, Zhou HM, Liu T, Wu LH, He XX*
- 1131 Reconstructing the portal vein through a posterior pancreatic tunnel: New choice for portal vein thrombosis during liver transplantation  
*Zhao D, Huang YM, Liang ZM, Zhang KJ, Fang TS, Yan X, Jin X, Zhang Y, Tang JX, Xie LJ, Zeng XC*
- 1141 Topological approach of liver segmentation based on 3D visualization technology in surgical planning for split liver transplantation  
*Zhao D, Zhang KJ, Fang TS, Yan X, Jin X, Liang ZM, Tang JX, Xie LJ*

**Observational Study**

- 1150 Can DKI-MRI predict recurrence and invasion of peritumoral zone of hepatocellular carcinoma after transcatheter arterial chemoembolization?  
*Cao X, Shi H, Dou WQ, Zhao XY, Zheng YX, Ge YP, Cheng HC, Geng DY, Wang JY*

**CASE REPORT**

- 1161 Cecocutaneous fistula diagnosed by computed tomography fistulography: A case report  
*Wu TY, Lo KH, Chen CY, Hu JM, Kang JC, Pu TW*
- 1169 Immunoglobulin G4-related disease in the sigmoid colon in patient with severe colonic fibrosis and obstruction: A case report  
*Zhan WL, Liu L, Jiang W, He FX, Qu HT, Cao ZX, Xu XS*

**ABOUT COVER**

Editorial Board Member of *World Journal of Gastrointestinal Surgery*, Anil Kumar Agarwal, FACS, FRCS (Hon), MBBS, MCh, MS, Director, Professor, Surgeon, Department of Gastrointestinal Surgery and Liver Transplant, GB Pant Institute of Postgraduate Medical Education and Research and Maulana Azad Medical College, Delhi University, New Delhi 110002, India. aka.gis@gmail.com

**AIMS AND SCOPE**

The primary aim of *World Journal of Gastrointestinal Surgery* (*WJGS, World J Gastrointest Surg*) is to provide scholars and readers from various fields of gastrointestinal surgery with a platform to publish high-quality basic and clinical research articles and communicate their research findings online.

*WJGS* mainly publishes articles reporting research results and findings obtained in the field of gastrointestinal surgery and covering a wide range of topics including biliary tract surgical procedures, biliopancreatic diversion, colectomy, esophagectomy, esophagostomy, pancreas transplantation, and pancreatectomy, etc.

**INDEXING/ABSTRACTING**

The *WJGS* is now abstracted and indexed in Science Citation Index Expanded (SCIE, also known as SciSearch®), Current Contents/Clinical Medicine, Journal Citation Reports/Science Edition, PubMed, PubMed Central, Reference Citation Analysis, China National Knowledge Infrastructure, China Science and Technology Journal Database, and Superstar Journals Database. The 2022 Edition of Journal Citation Reports® cites the 2021 impact factor (IF) for *WJGS* as 2.505; IF without journal self cites: 2.473; 5-year IF: 3.099; Journal Citation Indicator: 0.49; Ranking: 104 among 211 journals in surgery; Quartile category: Q2; Ranking: 81 among 93 journals in gastroenterology and hepatology; and Quartile category: Q4.

**RESPONSIBLE EDITORS FOR THIS ISSUE**

Production Editor: Rui-Rui Wu, Production Department Director: Xiang Li, Editorial Office Director: Jia-Ru Fan.

**NAME OF JOURNAL**

*World Journal of Gastrointestinal Surgery*

**ISSN**

ISSN 1948-9366 (online)

**LAUNCH DATE**

November 30, 2009

**FREQUENCY**

Monthly

**EDITORS-IN-CHIEF**

Peter Schemmer

**EDITORIAL BOARD MEMBERS**

<https://www.wjgnet.com/1948-9366/editorialboard.htm>

**PUBLICATION DATE**

October 27, 2022

**COPYRIGHT**

© 2022 Baishideng Publishing Group Inc

**INSTRUCTIONS TO AUTHORS**

<https://www.wjgnet.com/bpg/gerinfo/204>

**GUIDELINES FOR ETHICS DOCUMENTS**

<https://www.wjgnet.com/bpg/GerInfo/287>

**GUIDELINES FOR NON-NATIVE SPEAKERS OF ENGLISH**

<https://www.wjgnet.com/bpg/gerinfo/240>

**PUBLICATION ETHICS**

<https://www.wjgnet.com/bpg/GerInfo/288>

**PUBLICATION MISCONDUCT**

<https://www.wjgnet.com/bpg/gerinfo/208>

**ARTICLE PROCESSING CHARGE**

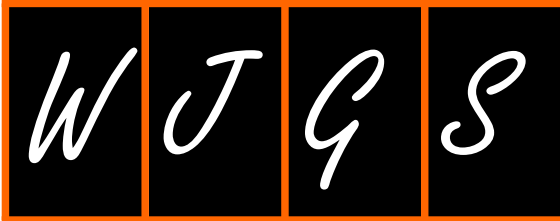
<https://www.wjgnet.com/bpg/gerinfo/242>

**STEPS FOR SUBMITTING MANUSCRIPTS**

<https://www.wjgnet.com/bpg/GerInfo/239>

**ONLINE SUBMISSION**

<https://www.f6publishing.com>



Observational Study

# Can DKI-MRI predict recurrence and invasion of peritumoral zone of hepatocellular carcinoma after transcatheter arterial chemoembolization?

Xin Cao, Hao Shi, Wei-Qiang Dou, Xin-Yao Zhao, Ying-Xin Zheng, Ya-Ping Ge, Hai-Chao Cheng, Dao-Ying Geng, Jun-Ying Wang

**Specialty type:** Radiology, nuclear medicine and medical imaging

**Provenance and peer review:**

Invited article; Externally peer reviewed.

**Peer-review model:** Single blind

**Peer-review report's scientific quality classification**

Grade A (Excellent): A  
Grade B (Very good): B, B  
Grade C (Good): 0  
Grade D (Fair): 0  
Grade E (Poor): 0

**P-Reviewer:** Elpek GO, Turkey; Pham TTT, Viet Nam; Shekouhi R, Iran

**Received:** April 18, 2022

**Peer-review started:** April 18, 2022

**First decision:** July 14, 2022

**Revised:** July 29, 2022

**Accepted:** September 21, 2022

**Article in press:** September 21, 2022

**Published online:** October 27, 2022



**Xin Cao, Hao Shi, Ya-Ping Ge, Hai-Chao Cheng, Jun-Ying Wang**, Department of Medical Imaging, The First Affiliated Hospital of Shandong First Medical University & Shandong Province Qianfoshan Hospital, Jinan 250014, Shandong Province, China

**Xin Cao, Dao-Ying Geng**, Department of Radiology, Huashan Hospital, Fudan University, Shanghai 200040, China

**Xin Cao, Dao-Ying Geng**, Center for Shanghai Intelligent Imaging for Critical Brain Diseases Engineering and Technology Research, Shanghai 200040, China

**Wei-Qiang Dou**, MR Research, GE Healthcare, Beijing 10076, China

**Xin-Yao Zhao**, Department of Radiology, Yantaishan Hospital, Yantai 264001, Shandong Province, China

**Ying-Xin Zheng**, Department of Magnetic Resonance Imaging, Zhangqiu District People's Hospital, Jinan 250200, Shandong Province, China

**Corresponding author:** Jun-Ying Wang, MD, Doctor, Department of Medical Imaging, The First Affiliated Hospital of Shandong First Medical University & Shandong Province Qianfoshan Hospital, No. 66 Jingshi Road, Jinan 250014, Shandong Province, China.

[jywang1120@163.com](mailto:jywang1120@163.com)

## Abstract

### BACKGROUND

Hepatocellular carcinoma (HCC) is a major cause of cancer-related mortality worldwide. Transcatheter arterial chemoembolization (TACE) has been performed as a palliative treatment for patients with HCC. However, HCC is easy to recur after TACE. Magnetic resonance imaging (MRI) has clinical potential in evaluating the TACE treatment effect for patients with liver cancer. However, traditional MRI has some limitations.

### AIM

To explore the clinical potential of diffusion kurtosis imaging (DKI) in predicting recurrence and cellular invasion of the peritumoral liver zone of HCC after TACE.

## METHODS

Seventy-six patients with 82 HCC nodules were recruited in this study and underwent DKI after TACE. According to pathological examinations or the overall modified response evaluation criteria in solid tumors (mRECIST) criterion, 48 and 34 nodules were divided into true progression and pseudo-progression groups, respectively. The TACE-treated area, peritumoral liver zone, and far-tumoral zone were evaluated on DKI-derived metric maps. Non-parametric *U* test and receiver operating characteristic curve (ROC) analysis were used to evaluate the prediction performance of each DKI metric between the two groups. The independent *t*-test was used to compare each DKI metric between the peritumoral and far-tumoral zones of the true progression group.

## RESULTS

DKI metrics, including mean diffusivity (MD), axial diffusivity (DA), radial diffusivity (DR), axial kurtosis (KA), and anisotropy fraction of kurtosis (FAk), showed statistically different values between the true progression and pseudo-progression groups ( $P < 0.05$ ). Among these, MD, DA, and DR values were higher in pseudo-progression lesions than in true progression lesions, whereas KA and FAk values were higher in true progression lesions than in pseudo-progression lesions. Moreover, for the true progression group, the peritumoral zone showed significantly different DA, DR, KA, and FAk values from the far-tumoral zone. Furthermore, MD values of the liver parenchyma (peritumoral and far-tumoral zones) were significantly lower in the true progression group than in the pseudo-progression group ( $P < 0.05$ ).

## CONCLUSION

DKI has been demonstrated with robust performance in predicting the therapeutic response of HCC to TACE. Moreover, DKI might reveal cellular invasion of the peritumoral zone by molecular diffusion-restricted change.

**Key Words:** Diffusion kurtosis imaging; Hepatocellular carcinoma; Transcatheter arterial chemoembolization; Recurrence

©The Author(s) 2022. Published by Baishideng Publishing Group Inc. All rights reserved.

**Core Tip:** This study demonstrated feasible performance and advantages of diffusion kurtosis imaging metrics (*i.e.*, mean diffusivity, axial diffusivity, radial diffusivity, axial kurtosis, and anisotropy fraction of kurtosis) in evaluating liver cancer and tumoral cell invasion of peritumoral zone between hepatocellular carcinoma progressive group and pseudo-progressive group after transcatheter arterial chemoembolization treatment.

**Citation:** Cao X, Shi H, Dou WQ, Zhao XY, Zheng YX, Ge YP, Cheng HC, Geng DY, Wang JY. Can DKI-MRI predict recurrence and invasion of peritumoral zone of hepatocellular carcinoma after transcatheter arterial chemoembolization? *World J Gastrointest Surg* 2022; 14(10): 1150-1160

**URL:** <https://www.wjgnet.com/1948-9366/full/v14/i10/1150.htm>

**DOI:** <https://dx.doi.org/10.4240/wjgs.v14.i10.1150>

## INTRODUCTION

Hepatocellular carcinoma (HCC) is a major cause of cancer-related mortality worldwide[1]. Unfortunately, most patients with HCC are diagnosed at the advanced stage and thus lose the opportunity for surgical resection. Transcatheter arterial chemoembolization (TACE), which blocks local blood supply of cancerous lesions to induce ischemia and necrosis with a mixture of chemotherapeutic agents[2], has been performed as a palliative treatment for patients with advanced stage HCC. With TACE, the survival rate and prognosis of patients with HCC could be significantly improved[3]. However, due to hypervascular feature and possibly established new collateral circulation[4], HCC is prone to being recurrent after TACE treatment. Thus, an accurate evaluation method is essential to help guide subsequent therapeutic planning for patients with HCC after TACE in clinical practice. In addition, after TACE, there may be microscopic changes prior to morphological changes in the peritumoral liver parenchyma zone of the true progression. While, no related studies have been conducted regarding this.

Magnetic resonance imaging (MRI) has clinical potential in evaluating the effect of TACE in patients with liver cancer[5]. However, anatomical MRI has some limitations. These include the following: (1) MRI signals are easily affected by various time points and different treatment methods; (2) para-

magnetic substances, such as hemorrhage, granulation tissue, protein components, and steatosis, present high signal on T1-weighted imaging (T1WI) and may interfere with the enhancement of recurring lesions; and (3) disordered collateral circulation in TACE area can lead to false-negative diagnosis in arterial enhancement measurement.

Diffusion MRI, as a promising method of measuring the diffusion behavior of water molecules, sensitively reflects the physiological and morphological changes of tissues[6]. Diffusion-weighted imaging (DWI) has been relatively stable to different treatment methods[7] and has shown higher diagnostic performance in liver cancer after TACE than contrast-enhanced MRI[8]. However, the DWI metric apparent diffusion coefficient, derived in mono-exponential model, tends to be affected by various factors, such as macromolecule concentration, viscosity, and capillary perfusion[9]. In contrast, diffusion kurtosis imaging (DKI), a relatively novel diffusion imaging technique describing the deviations of water molecules diffusing away from Gaussian distribution, enables the precise depiction of microstructural environment[10]. With the DKI-derived parameter mean kurtosis (MK), HCC lesions can be well distinguished between the true progression and pseudo-progression groups[11]. Moreover, together with another DKI metric, mean diffusivity (MD), MK can assess the therapeutic response to TACE in HCC[12]. Although the effectiveness of both MK and MD has been validated, the remaining DKI parameters including fractional anisotropy of kurtosis (FAk), axial and radial kurtosis (KA and KR), and axial and radial diffusivity (DA and DR) have not yet been investigated for their clinical potential on HCC diagnosis after TACE. In addition, whether there are microscopic or molecular level changes in the liver parenchyma around the surviving lesion needs to be investigated.

Therefore, this study aimed to systematically explore the clinical feasibility of all DKI-derived metrics in predicting recurrence and cellular invasion of the peritumoral liver zone of HCC after TACE.

## MATERIALS AND METHODS

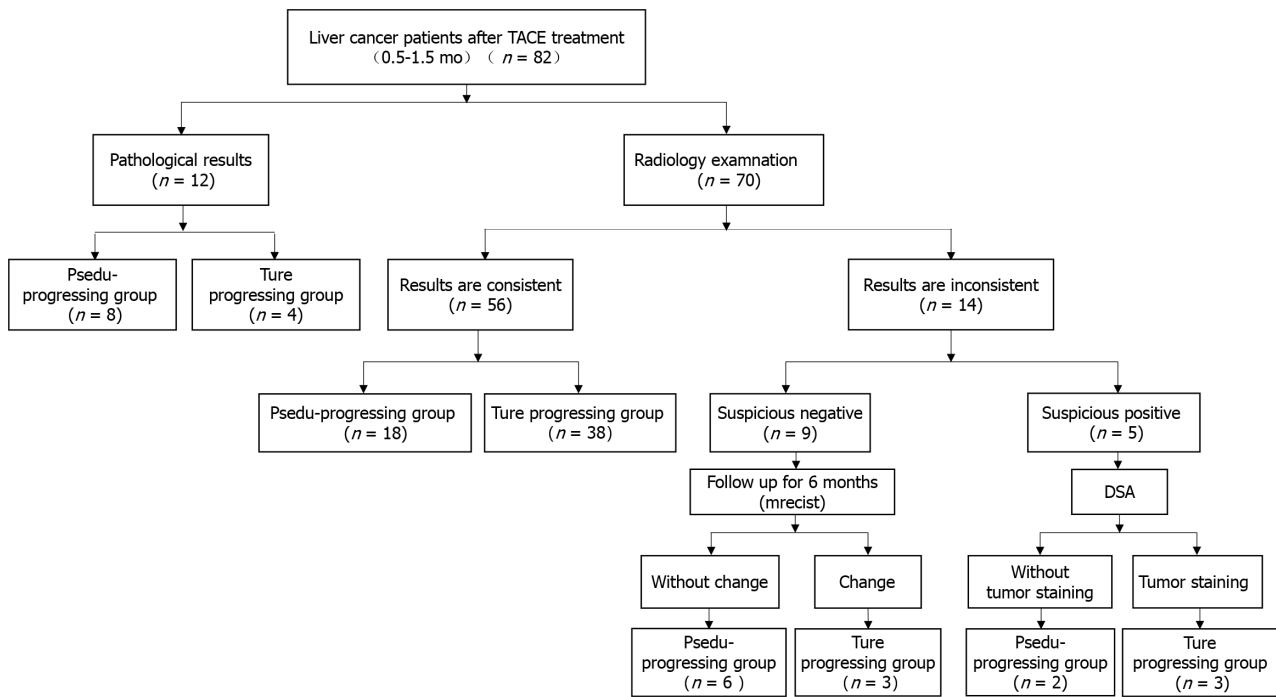
### Subjects

The local institutional review board approved this study, and each subject provided written informed consent. From January to May 2019, 76 patients (46 males *vs* 30 females; mean age, 55 years  $\pm$  12 years) with 82 HCC nodules were recruited in this study after receiving TACE treatment (1.4 mo  $\pm$  0.8 mo). Based on the pathological examination or the overall modified response evaluation criteria in solid tumors (mRECIST) criteria, 48 relapse/residual lesions and 34 stable and inactive lesions were divided into true progression and pseudo-progression groups, respective. The true progression was pathologically manifested as viable tumor cells in the foci, including primary liver cancer among the incisions, necrotic material, and granulomatous inflammation. The pseudo-progression was manifested as absence of the cancer cell infiltration in the operation area, only liver cirrhosis nodules, and some fibrous necrosis components (Figure 1).

According to the mRECIST criteria proposed by the American Association for the Study of Liver Diseases and European Association for the Study of the Liver and combined clinical indications, we considered the following lesions as true progression lesions[13]: (1) Progressive disease: Target lesion diameter increased by at least 20% on enhanced imaging compared with previous examination; (2) stable disease: Target lesion did not change; (3) partial response: The sum of initial lesion diameters in all target areas was reduced by at least 30%; (4) digital subtraction angiography (DSA): Lipiodol angiography found tumor staining in the focus area; and (5) alpha-fetoprotein (AFP) was significantly increased. However, if lesions met the following criteria, they were classified into the pseudo-progression group: (1) After TACE, DSA revealed that the focus was stable (no clear tumor blood vessels, tumor staining, clear arterial-venous/portal fistula, or vein-portal fistula); (2) after follow-up for a period of time (7.8 mo  $\pm$  0.5 mo), previous foci showed no signs of recurrence (all target lesions disappeared during the arterial enhancement phase of imaging); and (3) AFP was normal.

### Imaging acquisition

All MRI studies were performed using a 3T MRI scanner (Discovery MR750, GE, United States), with eight-channel abdomen coils employed. A respiratory-gated spin-echo echo-planar imaging DKI sequence was performed in the axial plane. The corresponding applied scan parameters were as follows: Repetition time (TR), 3333 ms; echo time (TE), 69.4 ms; slice thickness, 6 mm; slice spacing, 2.0 mm; field of view, 360 mm  $\times$  288 mm; and matrix size, 128  $\times$  128. In addition, five *b* values (400, 800, 1200, 1600, and 2000 s/mm<sup>2</sup>) and 15 directions at each *b* value were used. The total scan time was 10 min. Conventional MRI was also performed, with the following parameters: T1WI: TR 3.7 ms, TE 1.1 ms, and slice thickness 6 mm; T2WI: TR 2319.5 ms, TE 68.0 ms, and slice thickness 6.0 mm; FS-T2WI: TR 9000.0 ms, TE 81.0 ms, and slice thickness 6.0 mm; and DWI sequence: TR 5000 ms and TE 50.8 ms. Dynamic-enhanced MRI with gadopentetate dimeglumine, captured the arterial (20 s), venous (60 s), delayed (2 min) and hepatobiliary (45-120 min) phases. Gadolinium-diethylenetriamine penta-acetic acid of 15-20 mL was injected intravenously through the back of the hand at a rate of 2 mL/s.



DOI: 10.4240/wjgs.v14.i10.1150 Copyright ©The Author(s) 2022.

**Figure 1** Flowchart of patient enrollment. *n*: Number of cases; TACE: Transcatheter arterial chemoembolization; mRECIST: Modified response evaluation criteria in solid tumors; DSA: Digital subtraction angiography.

DSA was performed under guidance on a Toshiba rotary DSA (GEIGS530, United States) machine. All patients were approached *via* the femoral artery and routinely underwent skin preparation, disinfection, draping, and local anesthesia in the groin area. After the artery was successfully inserted, the guide wire and catheter sheath were sequentially inserted. The Cook 5-F RH tube was introduced to select the abdominal trunk or common hepatic angiography to observe the tumor staining.

### Data analysis

Two professional radiologists (Hansen and HC), with 30 and 10 years of experience in MRI assessment, respectively, independently recorded the imaging and clinical data of the true progression and pseudo-progression groups (Table 1). All acquired DKI images were examined on the workstation using vendor-supplied postprocessing software (GE AW4.6 advantage, United States). The corresponding mappings of DKI-derived parameters (*i.e.*, MD, DA, DR, MK, KA, KR, and FAK) were obtained. The two radiologists independently selected the regions of interest (ROIs) for TACE-treated area, peritumoral area (distance < 2 cm to the tumor), and long-distance area (distance > 5 cm) on anatomical DKI image at  $b = 0 \text{ s/mm}^2$  and then copied them on each of the DKI-derived parametric maps (Figure 2). Each expert selected two different ROIs and calculated the average value. All chosen ROIs of a circular or oval form were selected carefully to avoid necrotic area. Considering the inter-subject variation, all obtained values were standardized based on the following formulas:  $\text{Std}_{\text{pseudoprogession}} = \text{ROI (pseudo-progression lesion)}/\text{ROI (normal parenchyma)}$  and  $\text{Std}_{\text{progession}} = \text{ROI (progession lesion)}/\text{ROI (normal parenchyma)}$ .

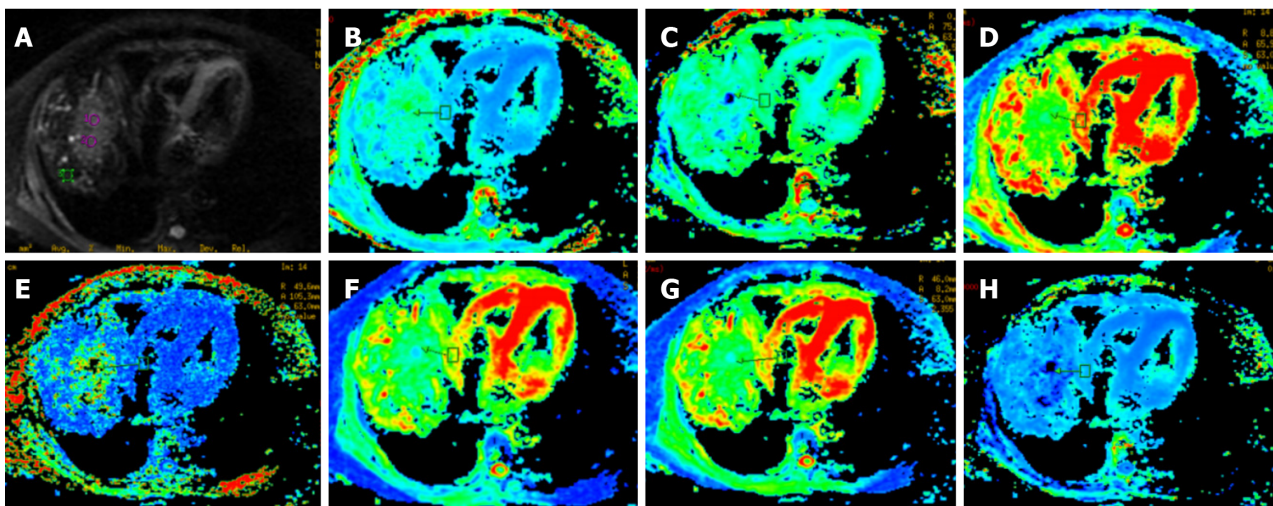
### Statistical analysis

All statistical analyses were performed using the Statistical Package for the Social Sciences version 22.0 statistical software. Intra-class correlation coefficient (ICC) analysis was performed to evaluate the inter-agreement of DKI parameter assessment by the two professional experts. The non-parametric *U* test and receiver operating characteristic (ROC) curve analysis were used to evaluate the differences and prediction performance of the DKI-derived parameters. The independent sample *t*-test was used to compare all DKI metrics in the peritumoral zone (distance < 2 cm) and the far-tumoral zone (distance > 5 cm) of the true progression group.  $P < 0.05$  was considered statistically significant.

**Table 1** Summary of clinical data of patients in true and pseudo-progressing groups

Characteristic	All cases (n = 82)	True group (n = 48)	Pseudo-group (n = 34)	P value
Age range (yr)	55 ± 12	50 ± 16	53 ± 14	0.745
Male/female (n)	46/30	26/18	20/12	0.402
AFP (ng/mL) (+/-)	49/33	47/1	2/32	0.001
Tumor-related characteristics				
Tumor size (cm)	4.0 ± 1.8	4.2 ± 1.6	2.7 ± 1.3	0.142
Enhancement (+/-)	50/32	46/2	4/30	0.006
DSA (+/-)	42/27	42/2	0/25	< 0.010
Resection (+/-)	10	9	1	-
TACE times (single/repeated)	26/56	4/44	22/12	< 0.011
Follow-up for > 6 mo (+/-)	39/33	39/0	0/33	< 0.001

AFP: Alpha-fetoprotein; DSA: Digital subtraction angiography; TACE: Transcatheter arterial chemoembolization.



DOI: 10.4240/wjgs.v14.i10.1150 Copyright ©The Author(s) 2022.

**Figure 2** Representative maps of trans catheter arterial chemoembolization-treated and recurrent hepatocellular carcinoma foci. The patient was a 46-year-old man with trans catheter arterial chemoembolization-treated and recurrent hepatocellular carcinoma foci. A: Diffusion map with  $b = 0$  s/mm<sup>2</sup>; B: Maps of mean kurtosis (MK); C: Maps of mean diffusivity (MD); D: Maps of radial kurtosis (KR); E: Maps of axial kurtosis (KA); F: Maps of axial diffusivity (DA); G: Maps of radial diffusivity (DR); H: Maps of anisotropy coefficient of kurtosis (FAK). In the first map (A), the region of interest (ROI) (1) corresponds to the arrow pointing to a new lesion. The peritumoral zone (distance < 2 cm) refers to ROI (2) (red circle), and far-tumoral zone (diameter > 5 cm) refers to ROI (3) (green square).

## RESULTS

### Clinical data analysis

Clinical data, including age, gender, and tumor-related characteristics, of patients in the true progression and pseudo-progression groups are summarized in [Table 1](#). There were significantly more patients in the true progression group than in the pseudo-progression group. Moreover, the true progression group had higher serum AFP level (> 200 ng/mL) ( $P < 0.05$ ) than the pseudo-progression group. In addition, significantly greater proportions of patients in the progression group showed typical enhancement (95.8%) and more or less tumor staining in lipiodol angiography (95.5%). In contrast, tumor size and age range were similar between the two groups ( $P > 0.05$ ). Among the 48 nodules in the progression group, 44 received repeated TACE, and the mean number of TACE sessions per nodule was 1-3. Four nodules underwent only a single course of TACE.

### Inter-observer agreement analysis

As shown in [Table 2](#), ICC analysis was utilised by two radiologists to assess the inter-agreement of each DKI parameter measurement on the TACE-treated region, peritumoral zone, and far-tumoral zone,

**Table 2 Evaluation of inter-observer agreement using intra-class correlation coefficient analysis**

	MK	MD	KA	KR	DA	DR	FAk
ROI (T)	0.86	0.85	0.80	0.83	0.76	0.78	0.62
ROI (N)	0.79	0.74	0.71	0.76	0.72	0.75	0.54
ROI (F)	0.70	0.73	0.69	0.68	0.64	0.70	0.50

FAk: Anisotropy coefficient of kurtosis; ROC: Receiver operating characteristic curve; MD: Mean diffusivity; MK: Mean kurtosis; KA: Axial kurtosis; KR: Radial kurtosis; DA: Axial diffusivity; DR: Radial diffusivity.

**Table 3 Diffusion kurtosis imaging derived metrics in true and pseudo-progressing lesions**

	MK	MD	KR	KA	DR	DA	FAk
N	0.60 ± 0.15	1.90 ± 0.65	0.55 ± 0.16	0.60 ± 0.13	1.88 ± 0.55	2.20 ± 0.63	0.10 ± 0.09
Y	0.71 ± 0.24	1.60 ± 0.45	0.65 ± 0.29	0.70 ± 0.15	1.4 ± 0.38	2.10 ± 0.60	0.32 ± 0.22
Std-N	0.68 ± 0.27	1.89 ± 0.58	0.70 ± 0.31	0.61 ± 0.16	2.01 ± 0.54	1.60 ± 0.42	0.54 ± 0.32
Std-Y	0.81 ± 0.23	0.91 ± 0.18	0.75 ± 0.24	1.03 ± 0.20	0.88 ± 0.22	0.92 ± 0.22	1.07 ± 0.78
P value	0.270	0.009	0.679	0.000	0.003	0.000	0.000

N = pseudo-progressing group; Y = true progressing group. FAk: Anisotropy coefficient of kurtosis; MD: Mean diffusivity; MK: Mean kurtosis; KA: Axial kurtosis; KR: Radial kurtosis; DA: Axial diffusivity; DR: Radial diffusivity.

separately. General excellent inter-agreement was confirmed by high ICC values. Among these, optimal measurement consistency was obtained in TACE-treated area for DKI-derived parameter values showing the best consistency, whereas the worst measurement consistency was found in the far-tumoral zone.

### Diffusion kurtosis imaging-derived parameter analysis

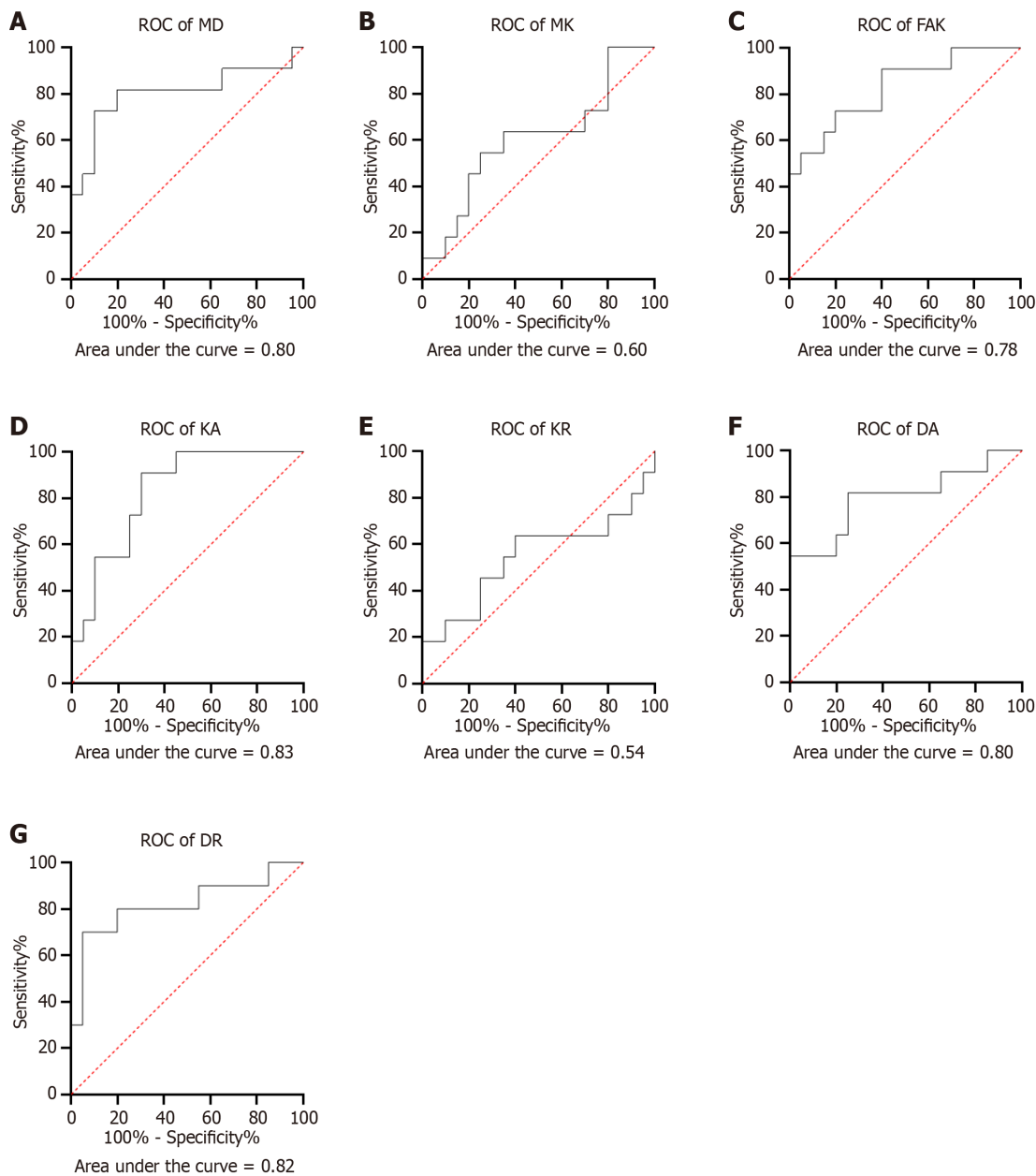
Compared to pseudo-progression inactive lesions, true progression recurrence lesions were associated with lower values of MD, DA, and DR ( $1.60 \pm 0.45 \times 10^{-3} \text{ mm/s}$  vs  $1.90 \pm 0.65 \times 10^{-3} \text{ mm/s}$ ,  $2.10 \pm 0.60 \times 10^{-3} \text{ mm/s}$  vs  $2.29 \pm 0.63 \times 10^{-3} \text{ mm/s}$ , and  $1.40 \pm 0.38 \times 10^{-3} \text{ mm/s}$  vs  $1.88 \pm 0.55 \times 10^{-3} \text{ mm/s}$ , respectively; Table 3). However, higher KA and FA values were found in the foci area of true progression lesions than of pseudo-progression lesions ( $0.70 \pm 0.15$  vs  $0.60 \pm 0.13$  and  $0.32 \pm 0.22$  vs  $0.10 \pm 0.09$ , respectively; Table 3). Moreover, ROC curve analysis was performed to compare the DKI-derived metrics in predicting recurrence performance (Figure 3). High AUC values were obtained for the parameters MD (0.80), FAk (0.78), KA (0.82), DA (0.82), and DR (0.80), whereas low ICC values were found in MK (0.6) and KR (0.54).

For the true progression group, DA and DR values were lower in the peritumoral zone (distance < 2 cm) than in the far-tumoral zone (distance > 5 cm) ( $2.11 \pm 0.52 \times 10^{-3} \text{ mm/s}$  vs  $2.44 \pm 0.59 \times 10^{-3} \text{ mm/s}$  and  $1.382 \pm 0.440 \times 10^{-3} \text{ mm/s}$  vs  $1.647 \pm 0.470 \times 10^{-3} \text{ mm/s}$ , respectively; Figure 4), whereas FAk and KA values showed opposite trends ( $0.309 \pm 0.110$  vs  $0.228 \pm 0.060$  and  $0.809 \pm 0.340$  vs  $0.783 \pm 0.120$ , respectively; Figure 3).

In addition, the MD values of the liver parenchyma (peritumoral and far-tumoral zones) were significantly lower in the true progression group than in the pseudo-progression group ( $0.866 \pm 0.330 \times 10^{-3} \text{ mm/s}$  vs  $1.677 \pm 0.630 \times 10^{-3} \text{ mm/s}$  and  $0.843 \pm 0.170 \times 10^{-3} \text{ mm/s}$  vs  $1.569 \pm 0.410 \times 10^{-3} \text{ mm/s}$ , respectively; Figure 4D).

## DISCUSSION

In this study, we explored the prediction performance of DKI for recurrence and cellular invasion of the peritumoral liver zone of HCC after TACE and further investigated the characteristics of the DKI-derived metrics between the true progression and pseudo-progression groups. Considering the high data consistency between the two experts, we found that most DKI metrics, including MD, DA, DR, KA, and FAk, showed statistically different values between the true progression and pseudo-progression groups ( $P < 0.05$ ). Moreover, for the true progression group, except the metrics MK and KR, all other parameters of the peritumoral liver zone (distance < 2 cm) were significantly different from those of the far-tumoral liver parenchyma (distance > 5 cm). Therefore, we concluded that DKI with derived



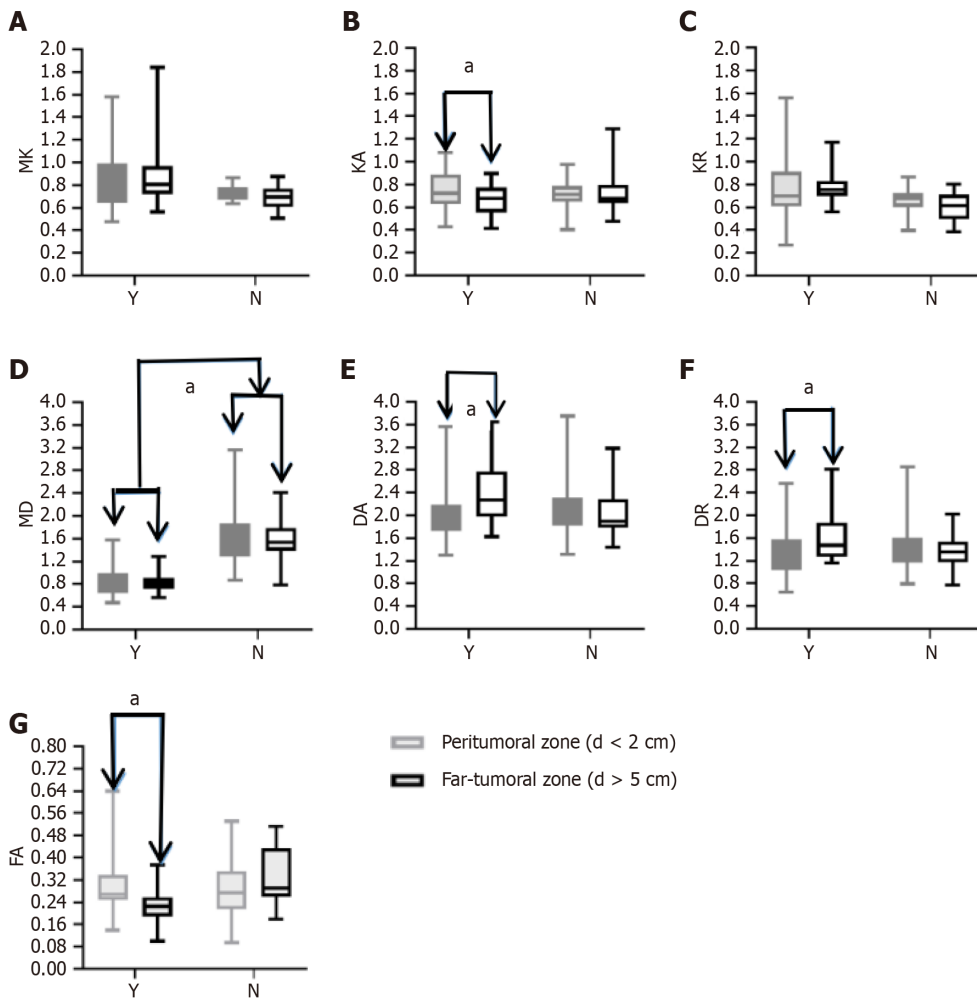
DOI: 10.4240/wjgs.v14.i10.1150 Copyright ©The Author(s) 2022.

**Figure 3 Receiver operating characteristic curves of diffusion kurtosis imaging metric in predicting recurrence.** AUC value greater than 0.7 indicates a higher diagnostic value. A: Mean diffusivity; B: Mean kurtosis; C: Anisotropy coefficient of kurtosis; D: Axial kurtosis; E: Radial kurtosis; F: Axial diffusivity; G: Radial diffusivity. FAK: Anisotropy coefficient of kurtosis; ROC: Receiver operating characteristic curve; MD: Mean diffusivity; MK: Mean kurtosis; KA: Axial kurtosis; KR: Radial kurtosis; DA: Axial diffusivity; DR: Radial diffusivity.

functional metrics showed advantages in assessing the therapeutic response of HCC to TACE and also provided robust performance in evaluating peritumoral zone invasion.

Except for FAK, especially in ROI (F) (far-tumoral zone, distance > 5 cm), all other DKI metrics showed excellent consistency measured by two professional experts. FAK has been shown to have a significant benefit in the central nervous system, where the nerve fibre structure exhibits full fractional anisotropy[14]. Nevertheless, the fibre structure in the liver lacks a defined fractional anisotropy, making it difficult to identify the specificity of FAK. Furthermore, Nasu *et al*[15] established the idea of "pseudo-fractional anisotropy artefact of the liver", which asserts that manual selection of ROI (F) is inherently subjective and can be influenced by heartbeat and breathing artifact. This artefact might be another explanation for low consistency of FAK.

Important findings in this study were that DKI parameters, including MD, DA, DR, KA, and FAK, showed statistical differences between the true progression and pseudo-progression groups ( $P < 0.05$ ). MD, DA, and DR values of pseudo-progression lesions were higher than those of true progression lesions, whereas KA and FAK values were higher in true progression lesions than in pseudo-progression lesions. Yuan *et al*[11] showed significant potential of DKI in assessing the therapeutic response of HCC



DOI: 10.4240/wjgs.v14.i10.1150 Copyright ©The Author(s) 2022.

**Figure 4** Box plots showing diffusion kurtosis imaging derived metrics of peritumoral zones between true and pseudo-progressing

groups. A: Mean kurtosis (MK); B: Axial kurtosis (KA); C: Radial kurtosis (KR); D: Mean diffusivity (MD); E: Axial diffusivity (DA); F: Radial diffusivity (DR); G: Anisotropy coefficient of kurtosis (FAK). <sup>a</sup> $P < 0.05$ ; the unit of MD, DA, and DR is  $10^{-3} \text{ mm}^2/\text{s}$ . N = pseudo-progressing group; Y = true progressing group. FAK: Anisotropy coefficient of kurtosis; MD: Mean diffusivity; MK: Mean kurtosis; KA: Axial kurtosis; KR: Radial kurtosis; DA: Axial diffusivity; DR: Radial diffusivity.

to TACE. Thus, they believed that MK is an effective biomarker in the assessment of HCC progression after TACE. This conclusion, however, is not fully consistent with our results. Compared with the pseudo-progression group with inactive foci after TACE, the normalized MK value of the true progression group with residual/recurrent foci was not higher. Since MK can reflect the complexity and density of tissues[16], high cell density usually shows high MK value. We hypothesized that after TACE, foci cells are swelling and experience degeneration or necrosis, while leads to a decreased cell density. Moreover, some low-activity tumor cells have been severely damaged in structure, but still retain the ability to metastasize and recur. This type of condition cannot be effectively screened out based on the characteristics of tissue density, leading to the absence of statistical difference of the MK value between the true progression and pseudo-progression groups. It is worth mentioning that KA in this study revealed certain sensitivity in assessing tumor recurrence. Follow-up studies should be further conducted to explore the underlying mechanism.

Additionally, the clinical potential of DKI in determining the invasion of peritumoral zone of the residual foci for the true progression group was assessed. We discovered that diffusion metrics (DA and DR) differed considerably between the far-tumoral zone (distance > 5 cm) and the peritumoral zone (distance < 2 cm). The peritumoral zone (distance < 2 cm) had lower DA and DR values than the far-tumoral zone (distance > 5 cm), indicating that microenvironmental alterations may occur in the peritumoral zone, which is close to residual/recurrent foci and may be sensitive in representing cancer cell infiltration. However, only KA revealed a larger value in the peritumoral zone than the far-tumoral zone among the three kurtosis coefficients (MK, KR, and KA).

Despite the fact that a variety of DKI implementations have investigated the correlations of MK and MD with fibrosis or liver function[17-20], no similar DKI findings have been published in these studies. Yoshimaru *et al*[17] investigated the relationship between MK and Child-Pugh score in 79 patients with varying degrees of hepatic decompensation and found a minor correlation. In comparison, Goshima *et al*

[18] investigated the relationship between MK and Child-Pugh score but found no association. There was also disagreement about whether MK or MD had a superior diagnostic effectiveness for liver fibrosis. In another study, Hu *et al*[19] concluded that MD correlated strongly with the degrees of liver fibrosis, and the parameter MK may provide complementary information. In contrast, Li *et al*[20] claimed that MK could best predict the liver fibrosis stage. In this study, we did not analyze the relationship between DKI parameters and liver fibrosis or function. However, the MD value of the liver parenchyma (peritumoral and far-tumoral zones) was lower in the true progression group than in the pseudo-progression group. Moreover, the MK value did not show any difference between the two groups. The results obtained in this study were more inclined to the view that MD has a higher sensitivity to detect the degree of fibrosis. We thus hypothesized that poor liver function and high grade of liver fibrosis may lead to poor prognosis and high recurrence rate.

There are some limitations in the present study. First, manual selection of active ROIs is inevitably subjective. According to the results of dynamic enhancement and DSA imaging, independent measurement by two experienced radiologists can minimize measurement errors. Second, DKI with 5 *b* values and 15 directions per *b* value currently takes a long time of 10 min for imaging. Third, each patient showed different fibrosis state and liver function. To minimize this effect, we selected the liver parenchyma far away from the focus area for standardization. Fourth, there was a lack of pathological examination of tumor changes before and after TACE treatment. Further studies with more pathologically confirmed cases are required to be conducted. Fifth, it was difficult to obtain the histological results for each lesion after TACE. Therefore, no pathological support could determine whether the surrounding liver parenchyma was invaded. Relevant pathological study is requested to further explore the relationship among DKI parameters, liver fibrosis, and peripheral infiltration.

---

## CONCLUSION

In conclusion, DKI metrics (MD, DA, DR, KA, and FAK) have been demonstrated with robust performance in predicting the therapeutic response of HCC to TACE and evaluating cellular invasion of the peritumoral zone.

## ARTICLE HIGHLIGHTS

### Research background

Transcatheter arterial chemoembolization (TACE) has been used to treat patients with hepatocellular carcinoma (HCC) as a palliative therapy. Nevertheless, HCC is prone to recur after TACE. Traditional anatomical MRI has certain limitations in assessing recurrence. Diffusion kurtosis imaging (DKI) provides a detailed depiction of the microstructural environment. Whether DKI-derived metrics can provide clinical feasibility in predicting HCC recurrence and cellular invasion of the peritumoral liver zone after TACE remains to be a concern.

### Research motivation

To investigate the clinical use of DKI in predicting recurrence and cellular invasion of HCC in the peritumoral liver zone after TACE.

### Research objectives

In this study, 76 patients with 82 hepatic cancer nodules were enrolled and underwent DKI after TACE. Forty-eight and 34 nodules were divided into two groups: True progression and pseudo-progression, respectively.

### Research methods

DKI-derived metric maps were used to assess the TACE-treated area, peritumoral liver zone, and far-tumoral zone. To compare the prediction performance of each DKI metric between the true progression and pseudo-progression groups, the non-parametric *U* test and receiver operating characteristic curve (ROC) analysis were performed. The independent *t*-test was utilized to compare each DKI metric between the peritumoral and far-tumoral zones in the true progression group.

### Research results

DKI metrics, including mean diffusivity (MD), axial diffusivity (DA), radial diffusivity (DR), axial kurtosis (KA), and anisotropy fraction of kurtosis (Fak), exhibited significantly different values between the true progression and pseudo-progression groups, respectively ( $P < 0.05$ ). Furthermore, the peritumoral zone had substantially different DA, DR, KA, and FAK values than the far-tumoral zone in the true progression group. Additionally, MD values of the liver parenchyma (peritumoral and far-

tumoral zones) were substantially lower in the true progression group compared to the pseudo-progression group ( $P < 0.05$ ).

### Research conclusions

DKI has been shown to predict the therapeutic response of HCC to TACE with high accuracy. Furthermore, DKI may indicate cellular invasion of the peritumoral zone by molecular diffusion-restricted change.

### Research perspectives

This study systematically investigated the clinical feasibility of all DKI-derived metrics in predicting recurrence and cellular invasion of the peritumoral liver zone of HCC after TACE, providing an accurate evaluation method to help guide subsequent therapeutic planning in clinical practice for patients with HCC after TACE.

---

## FOOTNOTES

**Author contributions:** Cao X and Wang JY designed and performed the research, and wrote the paper; Shi H designed the research and supervised the report; Zheng YX, Ge YP, and Cheng HC contributed to the analysis; Dou WQ, Zhao XY, and Geng DY provided clinical advice.

**Supported by** the Greater Bay Area Institute of Precision Medicine, No. KCH2310094; Shanghai Sailing Program, No. 22YF1405000; Research Startup Fund of Huashan Hospital Fudan University, No. 2021QD035; and Clinical Research Plan of SHDC, No. SHDC2020CR3020A.

**Institutional review board statement:** The study was conducted in accordance with the Declaration of Helsinki, and approved by the Institutional Review Board of Huashan Hospital and First Affiliated Hospital of Shandong First Medical University.

**Conflict-of-interest statement:** The authors declare no conflicts of interest for this article.

**Data sharing statement:** The data presented in this study are available on request from the corresponding author. The data are not publicly available due to protecting patient privacy.

**Open-Access:** This article is an open-access article that was selected by an in-house editor and fully peer-reviewed by external reviewers. It is distributed in accordance with the Creative Commons Attribution NonCommercial (CC BY-NC 4.0) license, which permits others to distribute, remix, adapt, build upon this work non-commercially, and license their derivative works on different terms, provided the original work is properly cited and the use is non-commercial. See: <https://creativecommons.org/licenses/by-nc/4.0/>

**Country/Territory of origin:** China

**ORCID number:** Xin Cao 0000-0003-3839-3076; Wei-Qiang Dou 0000-0003-0056-2014; Dao-Ying Geng 0000-0002-3585-6883; Jun-Ying Wang 0000-0003-3839-3207.

**S-Editor:** Chen YL

**L-Editor:** Wang TQ

**P-Editor:** Zhao S

---

## REFERENCES

- 1 **European Association for the Study of the Liver.** EASL Clinical Practice Guidelines: Management of hepatocellular carcinoma. *J Hepatol* 2018; **69**: 182-236 [PMID: 29628281 DOI: 10.1016/j.jhep.2018.03.019]
- 2 **Rognoni C,** Ciani O, Sommariva S, Facciorusso A, Tarricone R, Bhoori S, Mazzaferro V. Trans-arterial radioembolization in intermediate-advanced hepatocellular carcinoma: systematic review and meta-analyses. *Oncotarget* 2016; **7**: 72343-72355 [PMID: 27579537 DOI: 10.18632/oncotarget.11644]
- 3 **Sacco R,** Bertini M, Petruzzi P, Bertoni M, Bargellini I, Bresci G, Federici G, Gambardella L, Metrangola S, Parisi G, Romano A, Scaramuzzino A, Tumino E, Silvestri A, Altomare E, Vignali C, Capria A. Clinical impact of selective transarterial chemoembolization on hepatocellular carcinoma: a cohort study. *World J Gastroenterol* 2009; **15**: 1843-1848 [PMID: 19370781 DOI: 10.3748/wjg.15.1843]
- 4 **Ramsey DE,** Geschwind JF. Chemoembolization of hepatocellular carcinoma--what to tell the skeptics: review and meta-analysis. *Tech Vasc Interv Radiol* 2002; **5**: 122-126 [PMID: 12524642 DOI: 10.1053/tvir.2002.36418]
- 5 **Yu JS,** Kim JH, Chung JJ, Kim KW. Added value of diffusion-weighted imaging in the MRI assessment of perilesional tumor recurrence after chemoembolization of hepatocellular carcinomas. *J Magn Reson Imaging* 2009; **30**: 153-160 [PMID: 19370781 DOI: 10.1002/jmri.21843]

- 19557734 DOI: [10.1002/jmri.21818](https://doi.org/10.1002/jmri.21818)]
- 6 **Labeur TA**, Runge JH, Klompenhouwer EG, Klumpen HJ, Takkenberg RB, van Delden OM. Diffusion-weighted imaging of hepatocellular carcinoma before and after transarterial chemoembolization: role in survival prediction and response evaluation. *Abdom Radiol (NY)* 2019; **44**: 2740-2750 [PMID: [31069479](https://pubmed.ncbi.nlm.nih.gov/31069479/) DOI: [10.1007/s00261-019-02030-2](https://doi.org/10.1007/s00261-019-02030-2)]
  - 7 **Yang K**, Zhang XM, Yang L, Xu H, Peng J. Advanced imaging techniques in the therapeutic response of transarterial chemoembolization for hepatocellular carcinoma. *World J Gastroenterol* 2016; **22**: 4835-4847 [PMID: [27239110](https://pubmed.ncbi.nlm.nih.gov/27239110/) DOI: [10.3748/wjg.v22.i20.4835](https://doi.org/10.3748/wjg.v22.i20.4835)]
  - 8 **Kamel IR**, Bluemke DA, Ramsey D, Abusedera M, Torbenson M, Eng J, Szarf G, Geschwind JF. Role of diffusion-weighted imaging in estimating tumor necrosis after chemoembolization of hepatocellular carcinoma. *AJR Am J Roentgenol* 2003; **181**: 708-710 [PMID: [12933464](https://pubmed.ncbi.nlm.nih.gov/12933464/) DOI: [10.2214/ajr.181.3.1810708](https://doi.org/10.2214/ajr.181.3.1810708)]
  - 9 **Taouli B**, Tolia AJ, Losada M, Babb JS, Chan ES, Bannan MA, Tobias H. Diffusion-weighted MRI for quantification of liver fibrosis: preliminary experience. *AJR Am J Roentgenol* 2007; **189**: 799-806 [PMID: [17885048](https://pubmed.ncbi.nlm.nih.gov/17885048/) DOI: [10.2214/AJR.07.2086](https://doi.org/10.2214/AJR.07.2086)]
  - 10 **Wang J**, Dou W, Shi H, He X, Wang H, Ge Y, Cheng H. Diffusion kurtosis imaging in liver: a preliminary reproducibility study in healthy volunteers. *MAGMA* 2020; **33**: 877-883 [PMID: [32377906](https://pubmed.ncbi.nlm.nih.gov/32377906/) DOI: [10.1007/s10334-020-00846-4](https://doi.org/10.1007/s10334-020-00846-4)]
  - 11 **Yuan ZG**, Wang ZY, Xia MY, Li FZ, Li Y, Shen Z, Wang XZ. Diffusion Kurtosis Imaging for Assessing the Therapeutic Response of Transcatheter Arterial Chemoembolization in Hepatocellular Carcinoma. *J Cancer* 2020; **11**: 2339-2347 [PMID: [32127960](https://pubmed.ncbi.nlm.nih.gov/32127960/) DOI: [10.7150/jca.32491](https://doi.org/10.7150/jca.32491)]
  - 12 **Luo X**, Li Y, Shang Q, Liu H, Song L. Role of Diffusional Kurtosis Imaging in Evaluating the Efficacy of Transcatheter Arterial Chemoembolization in Patients with Liver Cancer. *Cancer Biother Radiopharm* 2019; **34**: 614-620 [PMID: [31560562](https://pubmed.ncbi.nlm.nih.gov/31560562/) DOI: [10.1089/cbr.2019.2878](https://doi.org/10.1089/cbr.2019.2878)]
  - 13 **Lencioni R**, Llovet JM. Modified RECIST (mRECIST) assessment for hepatocellular carcinoma. *Semin Liver Dis* 2010; **30**: 52-60 [PMID: [20175033](https://pubmed.ncbi.nlm.nih.gov/20175033/) DOI: [10.1055/s-0030-1247132](https://doi.org/10.1055/s-0030-1247132)]
  - 14 **Zhuo J**, Keledjian K, Xu S, Pampori A, Gerzanich V, Simard JM, Gullapalli RP. Changes in Diffusion Kurtosis Imaging and Magnetic Resonance Spectroscopy in a Direct Cranial Blast Traumatic Brain Injury (dc-bTBI) Model. *PLoS One* 2015; **10**: e0136151 [PMID: [26301778](https://pubmed.ncbi.nlm.nih.gov/26301778/) DOI: [10.1371/journal.pone.0136151](https://doi.org/10.1371/journal.pone.0136151)]
  - 15 **Nasu K**, Kuroki Y, Fujii H, Minami M. Hepatic pseudo-anisotropy: a specific artifact in hepatic diffusion-weighted images obtained with respiratory triggering. *MAGMA* 2007; **20**: 205-211 [PMID: [17960439](https://pubmed.ncbi.nlm.nih.gov/17960439/) DOI: [10.1007/s10334-007-0084-0](https://doi.org/10.1007/s10334-007-0084-0)]
  - 16 **Steven AJ**, Zhuo J, Melhem ER. Diffusion kurtosis imaging: an emerging technique for evaluating the microstructural environment of the brain. *AJR Am J Roentgenol* 2014; **202**: W26-W33 [PMID: [24370162](https://pubmed.ncbi.nlm.nih.gov/24370162/) DOI: [10.2214/AJR.13.11365](https://doi.org/10.2214/AJR.13.11365)]
  - 17 **Yoshimaru D**, Takatsu Y, Suzuki Y, Miyati T, Hamada Y, Funaki A, Tabata A, Maruyama C, Shimada M, Tobari M, Nishino T. Diffusion kurtosis imaging in the assessment of liver function: Its potential as an effective predictor of liver function. *Br J Radiol* 2019; **92**: 20170608 [PMID: [30358410](https://pubmed.ncbi.nlm.nih.gov/30358410/) DOI: [10.1259/bjr.20170608](https://doi.org/10.1259/bjr.20170608)]
  - 18 **Goshima S**, Kanematsu M, Noda Y, Kondo H, Watanabe H, Bae KT. Diffusion kurtosis imaging to assess response to treatment in hypervascular hepatocellular carcinoma. *AJR Am J Roentgenol* 2015; **204**: W543-W549 [PMID: [25905960](https://pubmed.ncbi.nlm.nih.gov/25905960/) DOI: [10.2214/AJR.14.13235](https://doi.org/10.2214/AJR.14.13235)]
  - 19 **Hu G**, Liang W, Wu M, Chan Q, Li Y, Xu J, Luo L, Quan X. Staging of rat liver fibrosis using monoexponential, stretched exponential and diffusion kurtosis models with diffusion weighted imaging- magnetic resonance. *Oncotarget* 2018; **9**: 2357-2366 [PMID: [29416777](https://pubmed.ncbi.nlm.nih.gov/29416777/) DOI: [10.18632/oncotarget.23413](https://doi.org/10.18632/oncotarget.23413)]
  - 20 **Li J**, Wang D, Chen TW, Xie F, Li R, Zhang XM, Jing ZL, Yang JQ, Ou J, Cao JM. Magnetic Resonance Diffusion Kurtosis Imaging for Evaluating Stage of Liver Fibrosis in a Rabbit Model. *Acad Radiol* 2019; **26**: e90-e97 [PMID: [30072289](https://pubmed.ncbi.nlm.nih.gov/30072289/) DOI: [10.1016/j.acra.2018.06.018](https://doi.org/10.1016/j.acra.2018.06.018)]



Published by **Baishideng Publishing Group Inc**  
7041 Koll Center Parkway, Suite 160, Pleasanton, CA 94566, USA  
**Telephone:** +1-925-3991568  
**E-mail:** [bpgoffice@wjgnet.com](mailto:bpgoffice@wjgnet.com)  
**Help Desk:** <https://www.f6publishing.com/helpdesk>  
<https://www.wjgnet.com>

